DOI: 10.58895/ksp/1000162754-8 erschienen in:
Proceedings. 33. Workshop Computational Intelligence - Berlin, 23. – 24. November 2023
DOI: 10.5445/KSP/1000162754 | https://www.ksp.kit.edu/site/books/e/10.5445/KSP/1000162754/

Data-driven identification of disturbances using a sliding mode observer

Ricarda-Samantha Götte, Jo Noel Klusmann, Julia Timmermann

Heinz Nixdorf Institute, Paderborn University
Fürstenallee 11
E-Mail: rgoette@hni.upb.de

1 Introduction

Sliding mode observers (SMOs) provide a robust tool for state estimation and give additional information about disturbances and model uncertainties [1]. Thus, they are frequently deployed for fault detection and analysis. However, analysis often contains only low-pass filtering without any further identification scheme [2]. Yet, characterizing disturbances may be advantageous not only for disturbance control to prevent any harm to the plant and maintain its desired behavior, but also to ensure a longer life cycle of mechanical components, e.g. by actively compensating for disturbances with eigenfrequencies. While our previous work [3, 4] focused on the joint estimation of states and model uncertainties in general, this contribution transfers the concepts to robust estimation. In particular, we demonstrate how to efficiently and even automatically receive dynamical representations for disturbances by a SMO, while also delivering correct state estimates. Ultimately, this insight can be utilized for disturbance control and model adaption.

2 Sliding Mode Observer

For the purpose of this contribution, a SMO is designed for the control of an inverted pendulum on a cart. The set up of the pendulum is displayed in Fig. 1a and its parameters are shown in Tab. 1b.

(a) Set up at our laboratory

Parameter	Value	SI Unit
mass m	0,654	kg
gravity g	9,81	m/s^2
length a	0,267	m
inertia J	0,0101	kg/m/s^2
damping d	0,001	N m s

(b) Table of parameters

Figure 1: Pendulum on a cart and its characteristics

Its dynamics are described by the following:

$$\begin{pmatrix} \dot{\varphi} \\ \ddot{\varphi} \\ \dot{s} \\ \ddot{s} \end{pmatrix} = \begin{pmatrix} \dot{\varphi} \\ \dfrac{am\cos(\varphi)\cdot u + mga\sin(\varphi) - d\dot{\varphi}}{J+ma^2} \\ \dot{s} \\ u \end{pmatrix}, \tag{1}$$

with φ denoting the angle, s the position of the cart and $\dot{\varphi}, \dot{s}$ the velocities, respectively. However, for simplicity we consider a second-order system in its nonlinear observability canonical form with dynamics f [5] to describe a SMO, since it can be easily adapted towards the pendulum on a cart. Then, the corresponding SMO takes the following form

$$\begin{aligned} \begin{pmatrix} \dot{\hat{x}}_1 \\ \dot{\hat{x}}_2 \end{pmatrix} &= \begin{pmatrix} \hat{x}_2 + \nu_1(e_y) \\ \hat{f}(\hat{x}_1, \hat{x}_2, u) + \nu_2(e_y) \end{pmatrix}, \\ \hat{y} &= \hat{x}_1, \\ e_y &= y - \hat{y} = x_1 - \hat{x}_1 = e_1, \end{aligned} \tag{2}$$

with $\hat{x}_1, \hat{x}_2$ denoting the estimated states, $\hat{f}$ representing the model of the system and e_y indicating the measurement error. Hence, the error dynamics with

$e_1 = x_1 - \hat{x}_1$ and $e_2 = x_2 - \hat{x}_2$ are deduced with Eq. (2) by

$$\begin{aligned} \dot{e}_1 &= e_2 + \nu_1(e_y), \\ \dot{e}_2 &= \Delta f + \nu_2(e_y). \end{aligned} \tag{3}$$

Δf is hereby the deviation between the system f and the model $\hat{f}$. The parameters k_i of the injection terms $\nu_i(e_y) = -k_i \operatorname{sign}(e_y)$ control the stability, effectiveness and convergence rate of the estimation. Especially, k_2 needs to be chosen such that $k_2 > |\Delta f|$ holds [1, 2] but guessing the maximal model deviation correctly often remains a challenge.

3 Data-driven disturbance identification

Since these injection terms $\nu_i(e_y) = -k_i \operatorname{sign}(e_y)$ are available at any time, we can utilize them for identifying the model deviation Δf. Assuming that the SMO is roughly well parameterized with design parameters k_i and has reached its sliding phase, we can not only expect $\dot{e}_y \to 0$ but also $\dot{e}_2 \to 0$. Thus, we receive $\Delta f = -\nu_2(e_y)$. Now instead of low-pass filtering Δf [2], which is usually the way to track potential disturbances, we seek for a physically interpretable representation of the disturbances besides capturing their dynamics. By this, we gain more insight into the disturbances and are able to e.g. compensate for these actively or analyze their effects regarding the life cycle of affected components such as actuators. Moreover, this information can be utilized for model adaption. Simply, assume a linear combination of n_θ suitable, physics-based terms stored within a library $\Psi \in \mathbb{R}^{n_\theta}$ that incorporate one's hypotheses which characteristics the disturbances may exhibit. Therefore, the following holds for Δf's approximation by the parameters $\theta \in \mathbb{R}^{n_\theta}$:

$$e_\theta = \Delta f - \theta^T \Psi(\hat{x}, u). \tag{4}$$

For useful insights into Δf, the interpretation error e_θ must tend towards zero, ideally for $t \to \infty$. Hence, the optimal $\hat{\theta}$ is found by minimizing

$$\arg\min_{\hat{\theta}} \int_0^t e_\theta^2 \mathrm{d}\tau = \int_0^t \left(-\nu_2(e_y) - \theta^T \Psi(\hat{x}, u)\right)^2 \mathrm{d}\tau, \tag{5}$$

whose solution is given by [6]

$$\hat{\theta} = \left(- \int_0^t \nu_2(e_y) \Psi(\hat{x}, u)^T \mathrm{d}\tau \right) \left[\int_0^t \Psi(\hat{x}, u) \Psi(\hat{x}, u)^T \mathrm{d}\tau \right]^{-1}. \tag{6}$$

By using an efficient, dynamic calculation for Ψ [6], the inversion of the library does not need to be computed completely within every time update. To account for changing characteristics and time-dependent behavior, the cost function can be averaged by a time factor if necessary.
However, choosing terms ψ_i for Ψ is difficult beforehand if no prior knowledge regarding the disturbances' characteristics is available. A solution to this challenge is to collect information regarding the disturbances, e.g. by a Fourier transformation for oscillations. Fig. 2 illustrates the Fourier transformation for the example used in Sec. 5, which identifies the three most important frequencies. Thus, using the Fourier transformation helps to identify the main frequencies that are then automatically included by trigonometric terms within Ψ as characteristics of Δf.

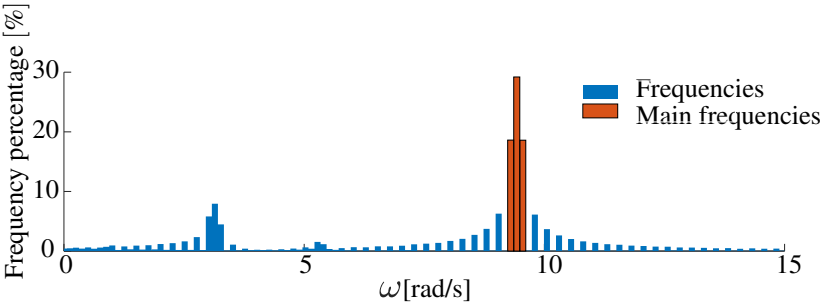

Figure 2: Fourier transformation to identify the main frequencies for choosing library terms ψ_i automatically

4 Results and outlook

To illustrate the effects of our proposed method, we present results from an open-loop scenario since it is easier to account for the outcomes without the

controller's influence. However, similar results have been obtained for closed-loop behavior using a linear quadratic controller combined with a DMOC optimal trajectory [7].
Forcing an external disturbance $\rho(t) = 4\sin(3\pi t + \pi/2)$ additional to the excitation $u(t) = \sin(\pi t + \pi/2)$ on the test bench at our laboratory, that affects the cart's position, we check if the proposed SMO automatically identifies the additional dynamics. Therefore, we compare two SMOs with libraries that are constructed differently. First, a library is set up by prior knowledge that contains the dynamics of $\rho(t)$. Thereafter, a library is constructed by the Fourier transform whose identified frequencies are utilized within it. Both libraries finally exhibit identical terms ψ_i to compare their performance, namely

$$\Psi(\hat{x}, u) = (\sin(\hat{\varphi}), \hat{\dot{\varphi}}, \mathrm{sign}(\hat{\dot{\varphi}}), \sin(\pi t + \pi/2), \sin(3\pi t + \pi/2), \sin(5\pi t + \pi/2))^T. \tag{7}$$

As Fig. 2 depicts the frequency of $\rho(t)$, namely $\omega_1 = 3\pi$, is identified correctly by the Fourier transformation. It also recognizes the frequency of the excitation $u(t)$ at $\omega_2 = \pi$. Using this information, Fig. 3 then shows excerpts regarding the convergence of the parameters $\hat{\theta}$ and the model deviation expressed by $\nu_2(e_y)$. If the library Ψ is set up by prior knowledge, the orange dashed signal in Fig. 3a shows that the deviation reduces much faster compared to when relevant terms for Ψ first need to be determined by a Fourier transformation which is illustrated by the blue dashed signal. However, in cases when we do not have any information regarding $\rho(t)$, this enables a fully automated identification of disturbances and features only slightly more convergence time due to the necessary collection of data that lasts in this case around $26s$. Note that it ultimately arrives at a similar level of error compared to when prior knowledge is used directly.

Considering the course of the parameters $\hat{\theta}$, both strategies show strong convergence rates, only varying in speed due to the data collection and analysis of the Fourier transformation. Yet, both converge to the same value and deliver consistent results, e.g. identifying the term $\psi(t) = \sin(3\pi t + \pi/2)$ as present within the disturbances and neglecting the term $\psi(t) = \sin(5\pi t + \pi/2)$ by convergence towards zero. However, it can be noticed that the identified parameter $\hat{\theta}_{\sin(3\pi+\pi/2)}$, which both strategies converge to, does not coincide

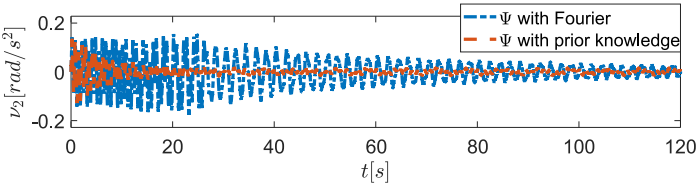

(a) Convergence of $\nu_2(t)$: It converges more slowly if no prior knowledge is used due to the necessary data collection for the Fourier transformation (blue) compared to when prior knowledge is applied (red).

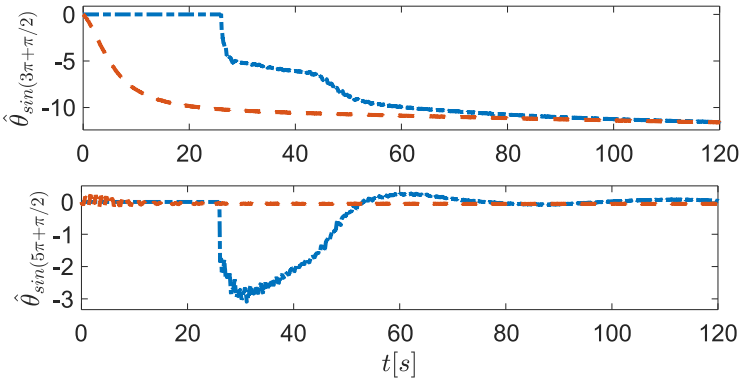

(b) Convergence of selected $\hat{\theta}$: Parts of $\rho(t)$ are identified correctly, although convergence rates vary due to how the library terms are determined.

Figure 3: Excerpts from the identification of Δf by prior and automatically chosen Ψ

with the amplitude of $\rho(t)$. This results from the effect that $\rho(t)$ acts directly on the control input $u(t)$. As Eq. (1) describes it holds $am\cos(\varphi)(J+ma^2)^{-1}\cdot u$. Due to the angle's oscillation around $-\pi$ as it can be seen later in Fig. 5, which results in $\cos(\varphi)\approx -1$, the factor tends to $am\cos(\varphi)(J+ma^2)^{-1}\approx 3$. Thus, both SMOs identify the overall amplitude of $\rho(t)$ with 12, assuming the factor rather belongs to the disturbance than to the control input.

Moreover, in addition to the decrease of $\nu_2(t)$, we verify if the SMOs identify the disturbance $\rho(t)$ correctly. Hence, Fig. 4 shows an excerpt of a comparison between the disturbance $\rho(t)$ and its approximation by the linear combination $\hat{\theta}^T\Psi(\hat{x},u)$ with the Fourier transformation once the parameters converged. It reveals that the approximation captures the disturbance well although some minor deviations can be recognized. Note that $\rho(t)$ is displayed with the factor

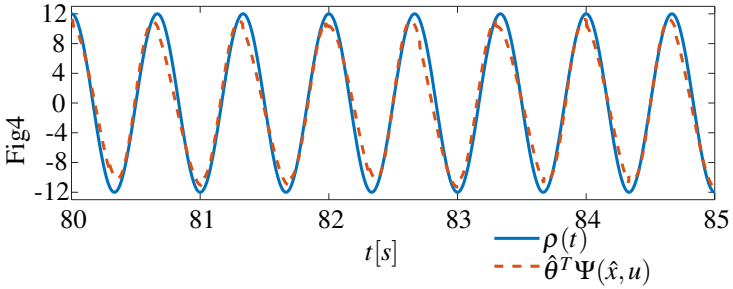

Figure 4: Excerpt from comparison of disturbance $\rho(t)$ and its approximation by $\hat{\theta}^T\Psi(\hat{x},u)$

acting on the control input, since the SMO assumes it acting on the disturbance.

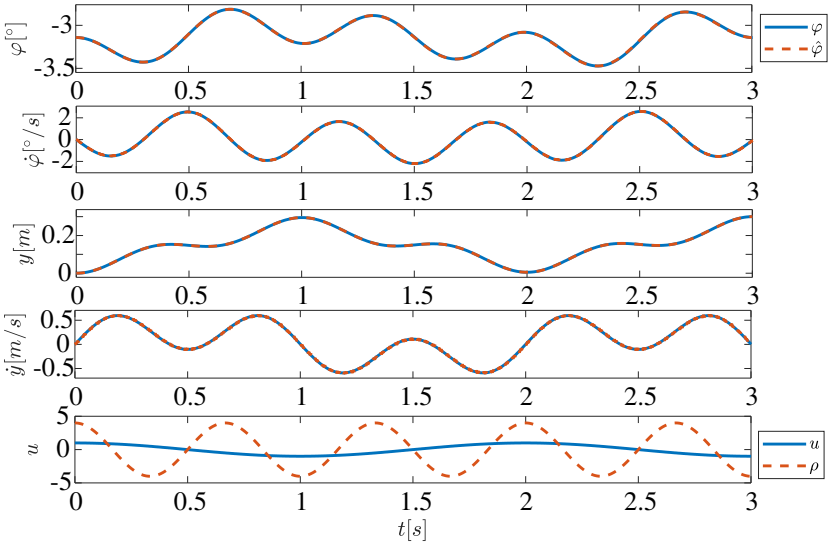

Figure 5: State estimation when the pendulum is excited by $u(t)$ and the observer gets additional disturbance $\rho(t)$

Since the injection term $v_2(t)$ decreases significantly over time and is already very low in the beginning of the estimation, the quality of the state estimation is expected to be high throughout. Fig. 5 confirms this impression by presenting the trajectories of the pendulum over time. Due to its good parameterization with k_i the sliding mode observer captures the pendulum's dynamical behavior

right from the beginning very well without any major estimation errors even though the disturbance is present and not yet fully identified.

In conclusion, this contribution showed the concept of joint estimation deployed within a sliding mode observer. It highlighted the advantages that result from disturbance identification and additionally presented the option to automatically receive candidate functions for the library by the Fourier transformation. Further, it convinced with a high quality of state estimation, while gaining more insight into present disturbances. Future research allows the usage of those strategies for intelligent fault management and provides a tool for online model adaption.

Acknowledgment

This work was developed in the junior research group DART, Paderborn University, and funded by the Federal Ministry of Education and Research of Germany under the funding code 01IS20052. The responsibility for the content of this publication lies with the authors.

References

[1] S. K. Spurgeon, "Sliding mode observers: a survey," *International Journal of Systems Science*, vol. 39, no. 8, pp. 751–764, 2008.

[2] Y. Shtessel, C. Edwards, L. Fridman, and A. Levant, *Sliding mode control and observation*, 1st ed. New York and Heidelberg: Birkhäuser, 2013.

[3] R.-S. Götte and J. Timmermann, "Estimating states and model uncertainties jointly by a sparsity promoting ukf," *IFAC-PapersOnLine*, vol. 1, no. 56, pp. 85–90, 2023.

[4] ——, "Approximating a laplacian prior for joint state and model estimation within an ukf," in *Presented and Published at IFAC World Congress 2023*, 2023.

[5] J. Adamy, *Nonlinear Systems and Controls*, 1st ed. Berlin, Heidelberg: Springer Berlin Heidelberg, 2022.

[6] J. Davila, L. Fridman, and A. Poznyak, "Observation and identification of mechanical systems via second order sliding modes," in *International Workshop on Variable Structure Systems, 2006. VSS'06*. IEEE, 2006, pp. 232–237.

[7] J. Timmermann, S. Khatab, S. Ober-Blöbaum, and A. Trächtler, "Discrete mechanics and optimal control and its application to a double pendulum on a cart," *IFAC Proceedings Volumes*, vol. 44, no. 1, pp. 10 199–10 206, 2011.